ELSEVIER

Journal of Hydrology 200 (1997) 24–39

Journal of Hydrology

ENSO and the natural variability in the flow of tropical rivers

Kishan N. Amarasekera, Robert F. Lee, Earle R. Williams, Elfatih A.B. Eltahir*

Ralph M. Parsons Laboratory, Department of Civil and Environmental Engineering, Massachusetts Institute of Technology, Cambridge, MA 02139, USA

Received 27 March 1996; revised 5 December 1996; accepted 5 December 1996

Abstract

This paper examines the relationship between the annual discharges of the Amazon, Congo, Paran á, and Nile rivers and the sea surface temperature (SST) anomalies of the eastern and central equatorial Pacific Ocean, an index of El Niño–Southern Oscillation (ENSO). Since river systems are comprehensive integrators of rainfall over large areas, accurate characterization of the flow regimes in major rivers will increase our understanding of large-scale global atmospheric dynamics. Results of this study reveal that the annual discharges of two large equatorial tropical rivers, the Amazon and the Congo, are weakly and negatively correlated with the equatorial Pacific SST anomalies with 10% of the variance in annual discharge explained by ENSO. Two smaller sub-tropical rivers, the Nile and the Paraná, show a correlation that is stronger by about a factor of 2. The Nile discharge is negatively correlated with the SST anomaly, whereas the Paraná river discharge shows a positive relation. The tendency for reduced rainfall/discharge over large tropical convection zones in the ENSO warm phase is attributed to global scale subsidence associated with major upwelling in the eastern Pacific Ocean. © 1997 Elsevier Science B.V.

Keywords: Tropical rivers; Flow variability; Sea surface temperature (SST); El Niño-Southern Oscillation (ENSO)

1. Introduction

The four major tropical rivers depicted in Fig. 1, the Amazon, Congo, Paraná, and Nile, drain approximately one-quarter of the world's land surface. These tropical rivers, by their size and location, have great impacts on the economies and populations of many countries.

* Corresponding author. Fax: +1 617 253 7462.

PII S0022-1694(96)03340-9

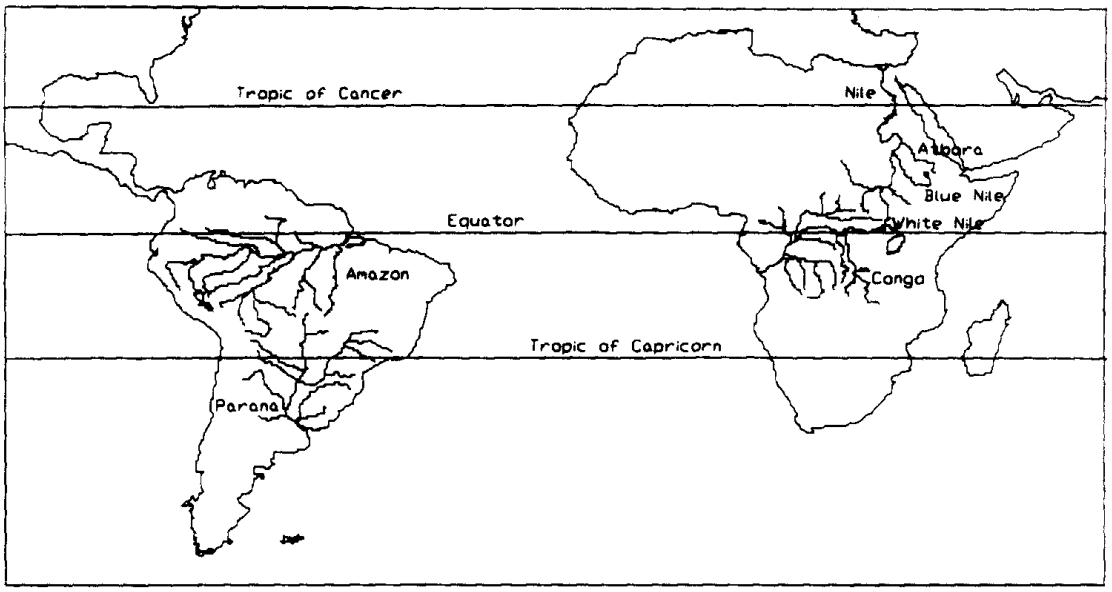

Fig. 1. Map of the rivers studied.

Accurate, long-term streamflow forecasting is vital for effective water resource management, and is therefore a tool of immense socio-economic significance, particularly in tropical regions. In addition, better characterization of river discharge patterns will lead to an increased understanding of global atmospheric dynamics, since streamflow is an index of precipitation integrated over drainage basins.

A large-scale coupled ocean–atmosphere oscillation in the Pacific Ocean, known as the El Niño–Southern Oscillation (ENSO), is related to inter-annual variations in precipitation and streamflow in several regions of the world. ENSO events are warming episodes of the eastern equatorial Pacific Ocean that influence the global climate on time scales of years to decades. It is also recognized that the ENSO temperature signal pervades the entire tropical belt (Hansen and Lebedeff, 1987). Recent studies indicate that ENSO events can be accurately predicted one to two years in advance using a physical model of the coupled ocean–atmosphere system (Cane et al., 1986; Chen et al., 1995). Therefore, the ability to predict flow patterns in rivers will be highly enhanced if a strong relationship between river discharge and ENSO exists, and is quantified.

Two different indices, sea surface temperature (SST) anomalies and the Southern Oscillation Index (SOI), are used to quantify ENSO. The SST anomaly is the sea surface temperature departure from the long-term mean, averaged over a well defined area of the eastern and central equatorial Pacific Ocean, and the SOI is the difference in the standardized sea level pressure between Tahiti and Darwin, also in the equatorial Pacific. El Niño events, which occur every 2–7 years, are associated with high SST anomalies and a correspondingly low SOI. The warm El Niño phase is characterized by elevated temperatures throughout the tropics (Hansen and Lebedeff, 1987). Conversely, La Niña events are episodes of low SST anomalies and high SOIs. This cold phase is characterized by suppressed temperatures throughout the tropics.

Due to the heterogeneous nature of rainfall, a large number of measurement stations are needed for accurate characterization of rainfall patterns over large areas. River systems act

as comprehensive integrators of precipitation over well defined drainage basins. Since the drainage areas of major rivers are quite expansive, river discharge is a useful index of the precipitation characteristics over areas where extensive direct measurements of rainfall are impractical. A recent study in Australia found a stronger relationship between streamflow variability and ENSO than between rainfall variability and ENSO (Chiew et al., 1995).

Significant correlations between large-scale regional precipitation patterns and ENSO episodes have been identified for several specific regions around the world (Ropelewski and Halpert, 1987). A negative relation was observed between the eastern equatorial Pacific SST anomalies and seasonal monsoon precipitation over India and Sri Lanka (Rasmusson and Carpenter, 1983; Parthasarathy and Pant, 1985; Parthasarathy et al., 1988; Kiladis and Sinha, 1991).

In an analysis to determine the relation between El Niño and the flow of the Nile River, it was observed that 25% of the natural variability in the annual discharge can be attributed to ENSO (Eltahir, 1996). In southeastern Australia, the annual discharges of the Murray–Darling River system were found to be inversely related to SST anomalies in the eastern tropical Pacific Ocean (Simpson et al., 1993). Several other studies have investigated the associations between ENSO events and streamflow in different world regions (Rao and Hada, 1990; Mechoso and Iribarren, 1992; Kahya and Dracup, 1993; Moss et al., 1994).

This paper describes a homogenized analysis of the relationship between the discharges of several major tropical rivers and ENSO, an extension of a similar analysis performed on the Nile River (Eltahir, 1996) and an earlier study on the Amazon (Richey et al., 1989). The rivers considered are the Amazon, Congo, Paraná, and the Blue Nile, White Nile and Atbara tributaries of the Nile. The Nile tributaries are analyzed in order to determine the contribution of each to the ENSO signature found in the variability of annual Nile discharges. Table 1 contains a brief comparison of some pertinent hydrological characteristics of these rivers.

Section 2 describes the methodology followed in this study, while Section 3 details our analysis of the relationship between ENSO and the discharge of each river. A discussion of the results is presented in Section 4, where the dependence on ENSO of flows in other rivers is also discussed in an attempt to develop a more systematic picture for the tropics. Our conclusions are summarized in Section 5.

Table 1

Hydrological characteristics of the Amazon, Congo, Paraná and Nile rivers (Milliman and Meade, 1983; Shea, 1986; as compiled by Russell and Miller, 1990)

River	Length (km)	Drainage area ($\times 10^6$ km^2)	Annual runoff (km^3)	Latitude extent of drainage basin	Annual precipitation (km^3)	Runoff/ catchment (m)	Precipitation/ catchment (m)
Amazon	6577	6.15	6300	4°N–18°S	12000	1.02	1.95
Congo	4375	3.82	1250	7°N–12°S	5600	0.33	1.47
Paraná	3740	2.60	470	16°S–34°S	3300	0.18	1.27
Nile	6648	2.96	83	3°S–32°N	1900	0.03	0.64

2. Methodology

The objective of this study is to determine the type and magnitude of the correlation that exists between the annual discharge of several major rivers and the phase of ENSO. The total discharge of each river over the 12-month seasonal cycle of flow is assumed to capture the long-term variability due to ENSO. The seasonal cycle of each river is defined as a 12-month period starting from the month of lowest average discharge for each year. The annual discharge is plotted against eight quarterly averages of the SST anomaly. These quarterly averages of mean monthly SST anomalies are used as the SST index of ENSO in this analysis. The quarters are chosen in such a manner that two quarters precede and follow the four quarters of the seasonal cycle of flow.

For each river, the average monthly discharge is calculated and then the seasonal cycle of flow and the annual flow volume are determined. Next, time series plots of the annual discharges are generated with El Niño warm phase years identified. In this paper, the following are considered to be the warm phase years: 1902, 1905, 1911, 1914, 1918, 1923, 1925, 1930, 1932, 1939, 1941, 1951, 1953, 1957, 1965, 1969, 1972, 1976 and 1982–83 (Rasmusson and Carpenter, 1982; Quinn et al., 1978). The 1982–83 episode was reported to be an extremely warm ENSO event (Gill and Rasmusson, 1983). Finally, scatter plots of the annual floods against the eight applicable quarters of the average SST anomaly are generated, and linear correlation coefficients between the data are calculated.

3. ENSO and flow in tropical rivers

The ENSO index used in this study is the average monthly SST anomaly in the eastern equatorial Pacific. This index consists of monthly SST variations from the long-term mean, averaged over the regions 6–2°N, 170–90°W; 2°N–6°S, 180–90°W; and 6–10°S, 150–110°W of the Pacific Ocean for the period 1872–1986. The data set was published as a homogenized monthly series of the mean SST anomaly (Wright, 1989).

3.1. The Amazon river

The Amazon River discharge is notable for its sheer magnitude (the largest in the world) and highly damped hydrograph. The river flow data for the Amazon are derived from the daily records of the stage of the Rio Negro at Manaus (lat. 3°S, long. 60°W) for the period 1904–85. The integrated runoff represented by the Manaus record covers 3×10^6 km^2 of the Andean and western Amazonian watershed (Richey et al., 1989). The mean annual discharge for the period on record is approximately 3000 km^3 (approximately half the discharge at the mouth of the Amazon). Fig. 2 depicts the yearly discharges of the Amazon, with the year immediately following a warm phase year identified by solid circles, and the mean annual discharge indicated by the dashed line. The Amazon River exhibits an annual cycle with a gradual increase in discharge from a minimum in November to a peak around June or July. The annual discharge of the river is therefore defined to be the integrated streamflow from November of the previous year to October of the year of interest.

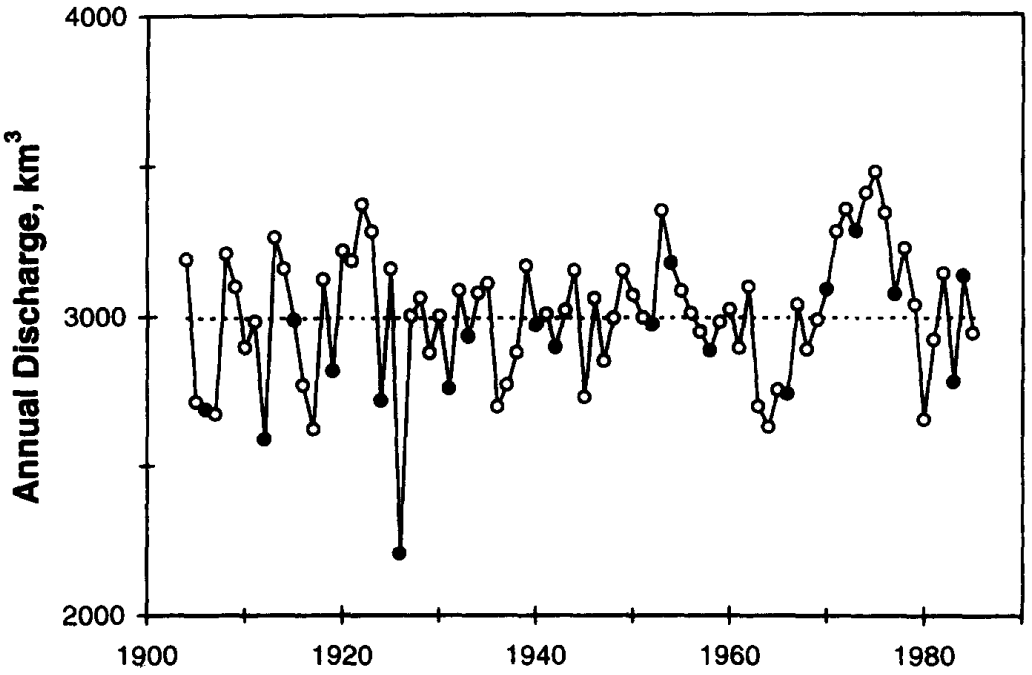

Fig. 2. Annual fluctuations in Amazon River discharges at Manaus for the years 1904–85. Years following El Niño years are marked with solid circles. The dashed line denotes the average annual discharge.

The results of a regression analysis of the data reveal that the Amazon discharge is weakly correlated with eight consecutive quarters of the SST index. Table 2 shows the result of the analysis for each quarter. A maximum correlation coefficient of negative 0.31 was calculated for the [Dec$^-$, Jan, Feb] quarter of the SST index. This result implies that approximately 10% of the variance in the annual flow of the Amazon River can be explained by the ENSO index for the [Dec$^-$, Jan, Feb] quarter. Fig. 3 is a scatter plot of the relation between the annual discharge of the Amazon and the SST index of ENSO for this quarter.

Table 2

Coefficients of correlation between the annual discharge of the Amazon River, and the SST anomaly in the eastern Pacific Ocean averaged for eight quarters. A negative (positive) sign following any month indicates that the month was from the year preceding (following) the year of interest

Quarter of the year	Correlation coefficient
Jun$^-$, Jul$^-$, Aug$^-$,	+0.01
Sep$^-$, Oct$^-$, Nov$^-$	−0.28
Dec$^-$, Jan, Feb	−0.31
Mar, Apr, May	−0.31
Jun, Jul, Aug	−0.16
Sep, Oct, Nov	−0.07
Dec, Jan$^+$, Feb$^+$	+0.04
Mar$^+$, Apr$^+$, May$^+$	+0.04

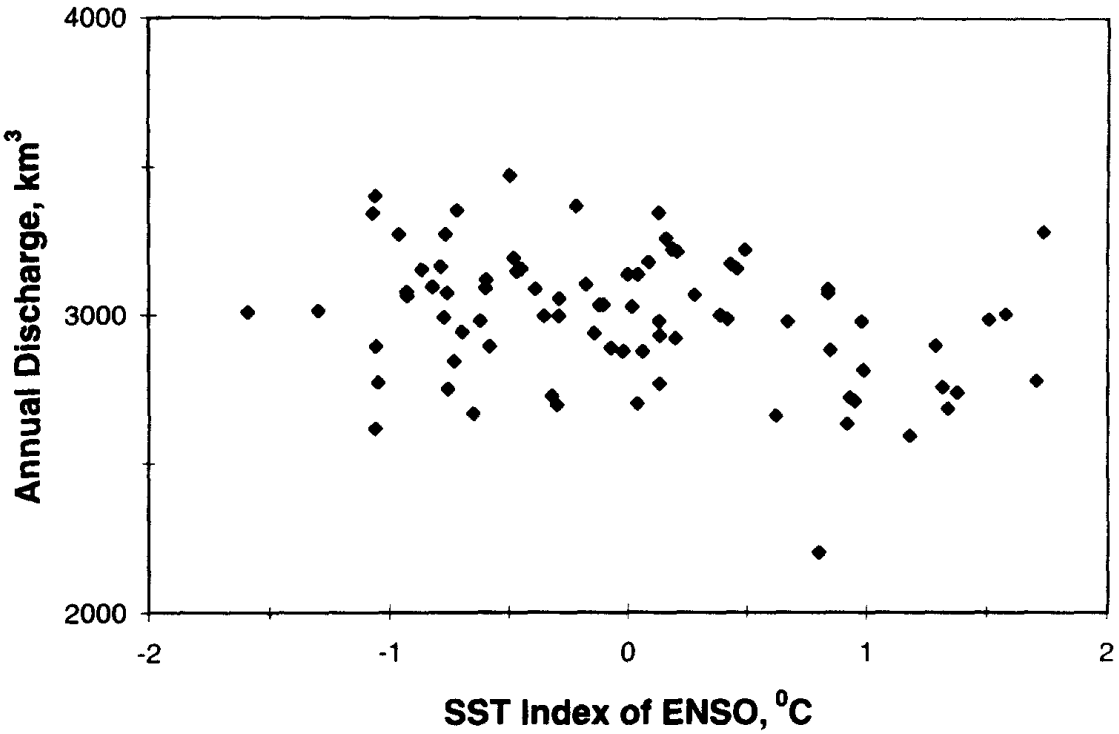

Fig. 3. Scatter plot of the relation between the annual discharge of the Amazon River and the SST index of ENSO for the months of Dec^{-}, Jan and Feb. The coefficient of correlation is negative 0.31.

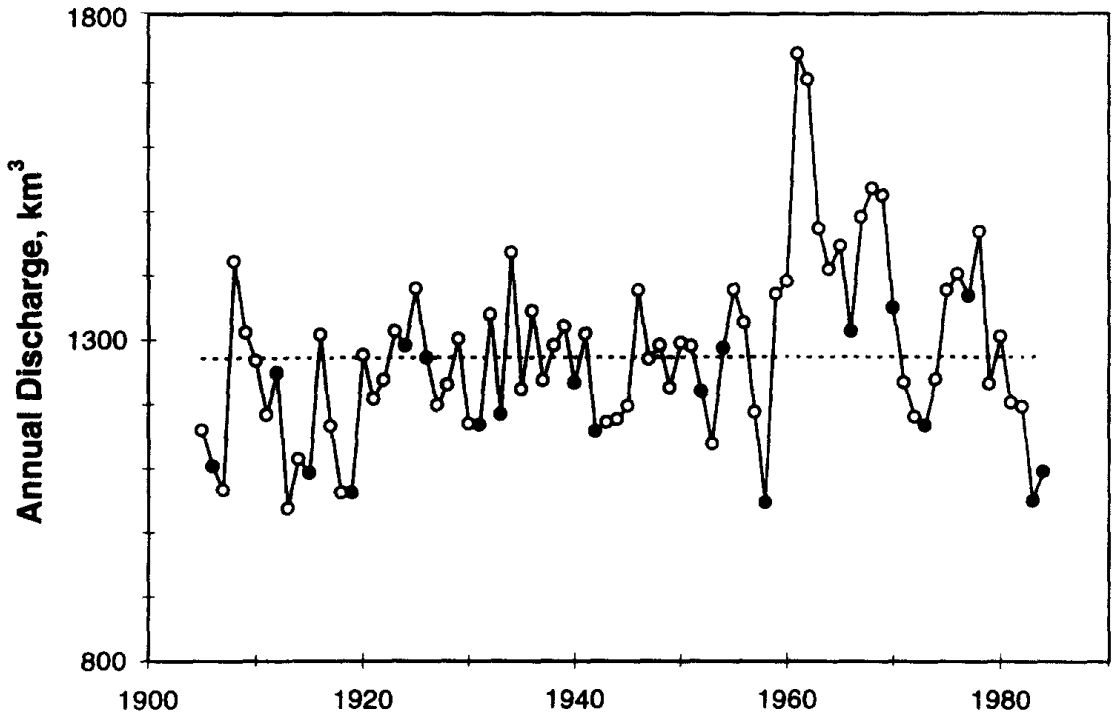

Fig. 4. Annual fluctuations in Congo River discharges at Kinshasa for the years 1905–85. Years following El Niño years are marked with solid circles. The dashed line denotes the average annual discharge.

3.2. The Congo river

The discharge data for the Congo River are monthly mean values derived by applying a discharge rating curve to the daily river stage at Kinshasa, Zaire (lat. 4°N, long. 15°E). The area of the Congo basin covered by the discharge data is approximately 3.8×10^6 km^2. The annual discharge of the Congo is plotted in Fig. 4 for the period 1905–85, with solid circles indicating the year immediately following a warm phase year. The discharge can be described as relatively stable except for the unusually high floods that lasted for a decade during the 1960s. The average annual flow of 1270 km^3 is indicated by the dashed line in the figure. Since the Congo River basin lies directly on the equator, it exhibits two seasonal floods per year. The smaller of the two floods has its peak in May and the more prominent flood peaks in December.

The annual discharge of the Congo River is defined as the total volume of flow from August of the year of interest to July of the following year. Correlation coefficients for the eight consecutive quarters correlated with the annual discharge are shown in Table 3. The SST index for the [Mar, Apr, May] quarter gives the highest correlation, with 10% of the variance in the annual flow due to ENSO. Fig. 5 shows the scatter plot of March to May SST index against annual river discharge.

3.3. The Paraná River

The Paraná River basin encompasses an area of 2.6×10^6 km^2 in Argentina, Brazil and Paraguay, and is the second largest drainage basin in South America. It is considered to be the most important basin of the La Plata basin system due to its discharge area and overall length. The Paraná River discharge data consist of the monthly flow at two locations, Posadas (lat. 27°S, long. 56°W) and Corrientes (lat. 27°S, long. 59°W), for the years 1902–92. Posadas and Corrientes are located upstream and downstream, respectively, of the confluence of the Paraguay and the Paraná rivers. Fig. 6 depicts the annual discharge of the Paraná at Corrientes, with the year following each warm phase year identified by a solid

Table 3

Coefficients of correlation between the annual discharge and the sum of discharge of October and November of the Congo River and the SST anomaly in the eastern Pacific Ocean averaged for eight quarters. A negative (positive) sign following any month indicates that the month was from the year preceding (following) the year of interest

Quarter of the year	Correlation coefficient annual flow
Sep$^-$, Oct$^-$, Nov$^-$	–0.24
Dec$^-$, Jan, Feb	–0.24
Mar, Apr, May	–0.31
Jun, Jul, Aug	–0.18
Sep, Oct, Nov	–0.11
Dec, Jan$^+$, Feb$^+$	–0.14
Mar$^+$, Apr$^+$, May$^+$	–0.16
Jun$^+$, Jul$^+$, Aug$^+$	+0.06

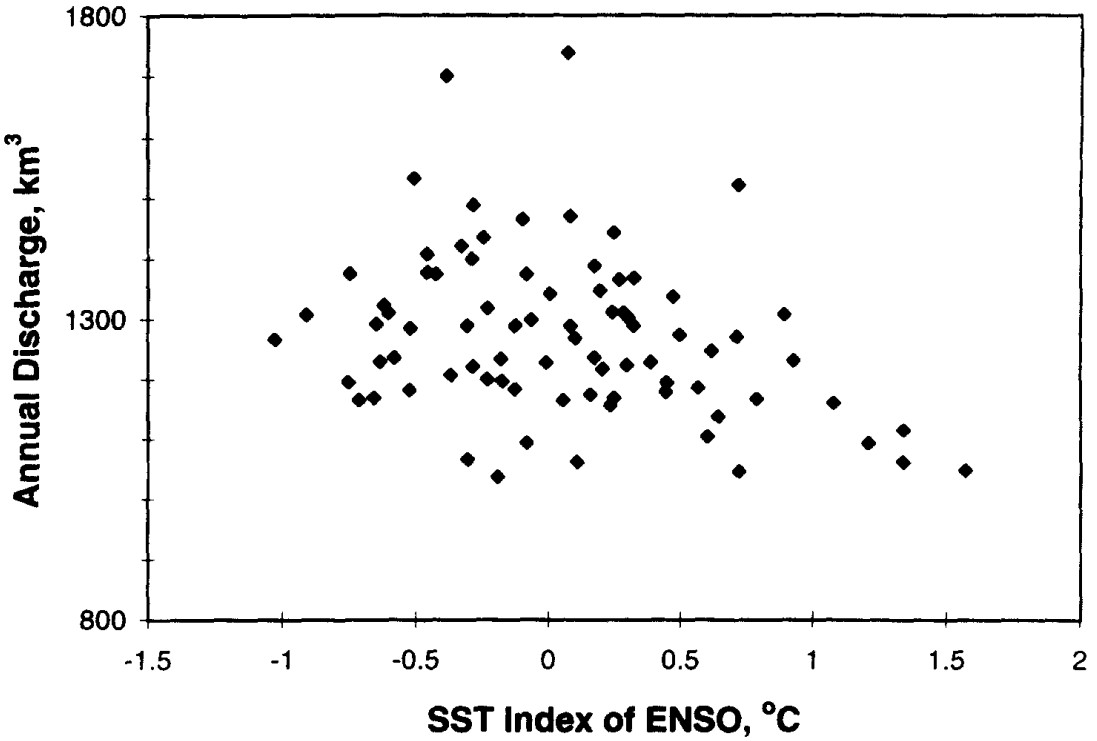

Fig. 5. Scatter plot of the relation between the annual discharge of the Congo River and the SST index of ENSO for the months of Mar, Apr, May. The coefficient of correlation is negative 0.31.

circle. The plot shows that a year following an ENSO event generally produces a higher than average flood. This trend was also observed at Posadas (not shown). While the long term mean annual discharge at Corrientes is 510 km^3, shown in Fig. 6 by the dashed line, the average discharge at Posadas is 390 m^3. The Paraná exhibits a seasonal cycle of a single peak with a long recession. High water occurs from December to April, peaking in March. Low discharge occurs in August and September.

Correlation coefficients obtained from a regression analysis between the annual discharge and eight consecutive quarters of the SST Index are shown in Table 4. The maximum percentage of variance in the annual discharge of the Paraná that can be explained by ENSO is 18% at Posadas and 19% at Corrientes for the [Dec$^-$, Jan, Feb] quarter. A scatter plot of the annual discharge at Corrientes versus the SST index for this quarter is presented in Fig. 7.

3.4. The Nile and its tributaries

The Nile River is formed by the confluence of the Blue and the White Nile at Khartoum in Sudan (lat. 15°S, long. 32.5°E), and the Atbara River joins the Nile approximately 500 km further downstream. The Blue Nile and Atbara rivers originate in the Ethiopian plateau, where positive pressure anomalies were observed to be positively correlated with the annual surface pressure at Darwin (Trenberth and Shea, 1987), and hence ENSO events. Since negative local pressure anomalies are associated with enhanced precipitation, a strong ENSO signal is expected in the annual Blue Nile and Atbara

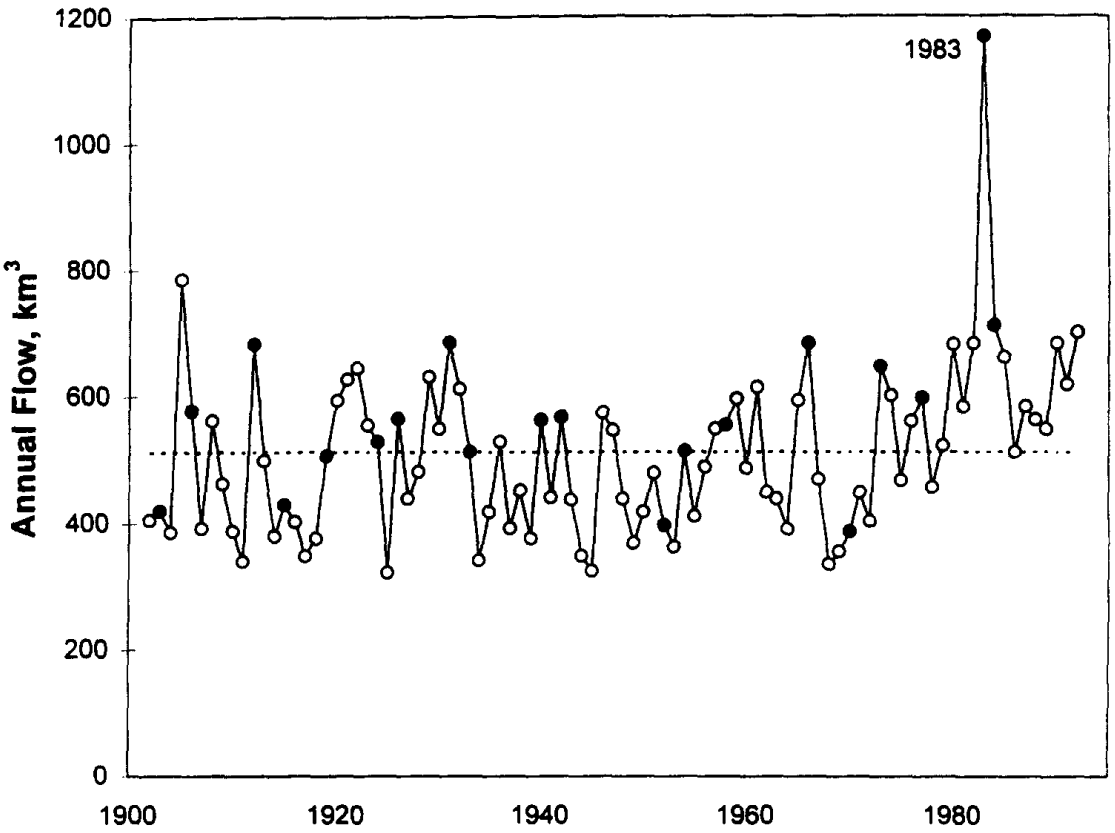

Fig. 6. Annual fluctuations in Paraná River discharges at Corrientes for the years 1902–92. Years following El Niño years are marked with solid circles. The dashed line denotes the average annual discharge. The anomalously large 1983 flood is also identified.

river discharges. The White Nile, however, flows through the equatorial lakes and marshes in the Sudd region, and is highly damped and expected to show very little association with ENSO. Therefore, the relationships between the annual discharges of the three major Nile tributaries and the SST index are analyzed in order to determine the contribution these

Table 4

Coefficients of correlation between the annual discharge of the Paraná River measured at Posadas and Corrientes, and the SST anomaly in the eastern Pacific Ocean averaged for eight quarters. A negative (positive) sign following any month indicates that the month was from the year preceding (following) the year of interest

Quarter of the year	Correlation coefficients: annual flow	
	Posadas	Corrientes
Mar$^-$, Apr$^-$, May$^-$	+0.16	+0.20
Jun$^-$, Jul$^-$, Aug$^-$	+0.38	+0.38
Sep$^-$, Oct$^-$, Nov$^-$	+0.41	+0.41
Dec$^-$, Jan, Feb	+0.43	+0.44
Mar, Apr, May	+0.38	+0.41
Jun, Jul, Aug	+0.19	+0.19
Sep, Oct, Nov	+0.14	+0.01
Dec, Jan$^+$, Feb$^+$	+0.003	+0.01

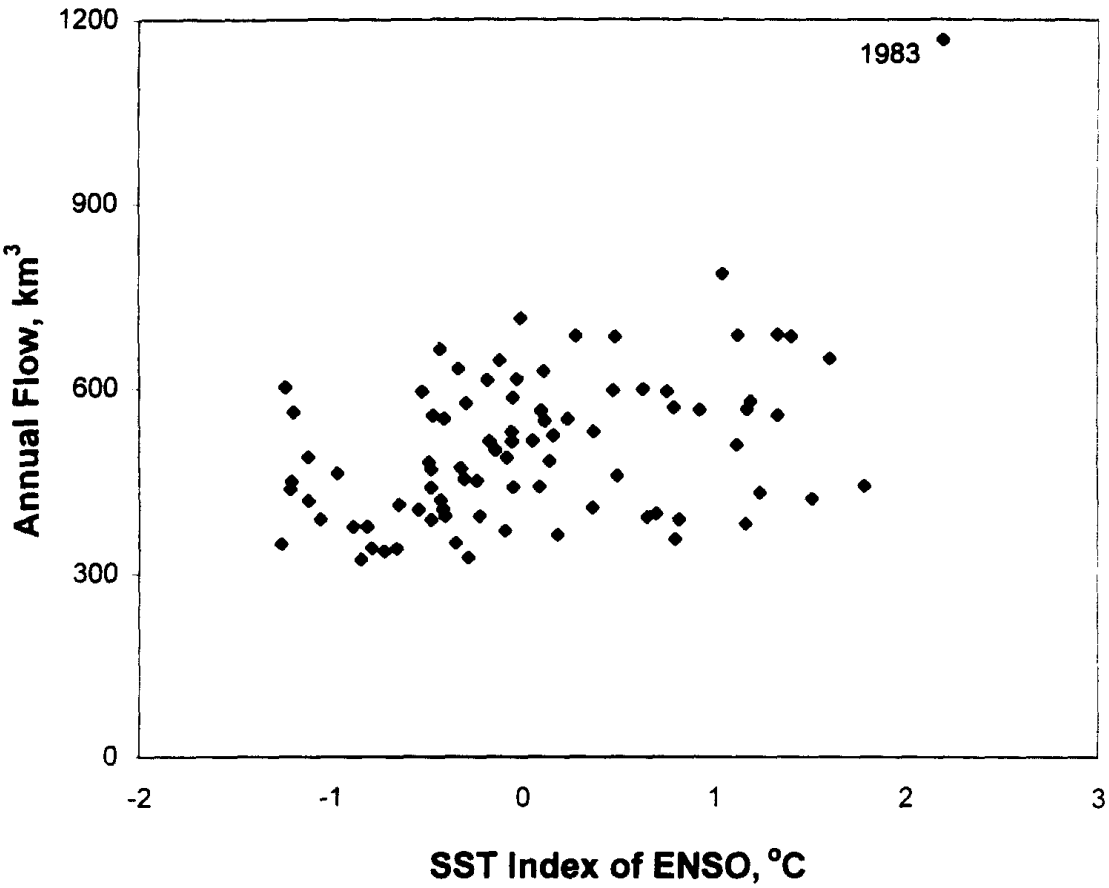

Fig. 7. Scatter plot of the relation between annual discharges of the Paraná River at Corrientes and the SST indices of ENSO for the months of Dec$^-$, Jan and Feb. The coefficient of correlation is positive 0.44. The anomalously large 1983 flood is also identified as the outlier.

Table 5

Coefficients of correlation between the annual discharges of the Nile, Blue Nile and Atbara rivers and the SST anomaly in the eastern Pacific Ocean averaged for eight quarters. A negative (positive) sign following any month indicates that the month was from the year preceding (following) the year of interest

Quarter of the year	Correlation coefficients			
	Nile	Blue Nile	Atbara	White Nile
Sep$^-$, Oct$^-$, Nov$^-$	−0.22	−0.14	−0.19	−0.08
Dec$^-$, Jan, Feb	−0.23	−0.14	−0.17	−0.14
Mar, Apr, May	−0.37	−0.27	−0.32	−0.20
Jun, Jul, Aug	−0.44	−0.44	−0.47	−0.05
Sep, Oct, Nov	−0.44	−0.44	−0.45	−0.07
Dec, Jan$^+$, Feb$^+$	−0.51	−0.47	−0.47	−0.13
Mar$^+$, Apr$^+$, May$^+$	−0.36	−0.29	−0.36	−0.08
Jun$^+$, Jul$^+$, Aug$^+$	−0.02	−0.01	−0.07	+0.18

tributaries make to the ENSO signature in the Nile discharge. Table 5 contains the correlation coefficients calculated between the Nile discharge and the SST index for the years 1912–72.

3.4.1. The Blue Nile and Atbara rivers

Fig. 8 shows a time series plot of the annual discharge of the Blue Nile and Atbara rivers, with the El Niño years marked by solid symbols (Shahin, 1985). The long-term average annual discharge of the Blue Nile is 50 km^3, approximately 60% of the annual Nile flow. The Atbara River contributes about 15% (12 km^3) of the Nile flow each year. The plot shows that ENSO years are associated with lower than average discharge in these two tributaries. The seasonal cycle of discharge for the Blue Nile is defined from May of the year of interest to April of the following year, while the Atbara River discharge has a strong seasonal variation, with low discharge from February to May, and peak flow occurring in August and September. Regression analysis of the Blue Nile annual discharge data reveals that the [Dec, Jan^+, Feb^+] quarter of SST index showed the highest correlation coefficient of negative 0.47. For the Atbara River, a maximum correlation coefficient of negative 0.47 was observed for the [Jun, Jul, Aug] quarter of SST. Table 5 contains the correlation coefficients for the eight consecutive quarters. Thus, approximately 22% of the annual variance of the Blue Nile and Atbara discharges can be attributed to ENSO. This is

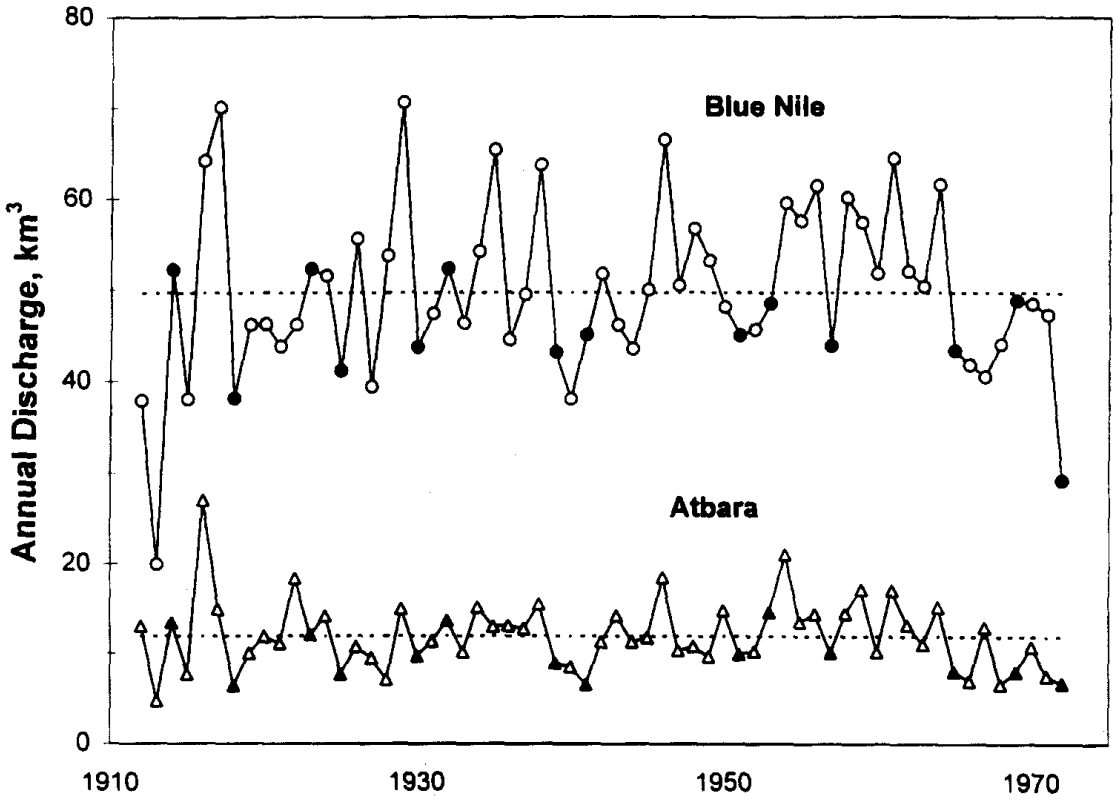

Fig. 8. Annual fluctuations in the Blue Nile and Atbara rivers for the years 1912–72. El Niño years are marked with solid symbols; dashed lines denote the average annual discharges of each river.

consistent with the previous calculation that 25% of the variance in the Nile annual discharge is due to ENSO (Eltahir, 1996).

3.4.2. The White Nile river

The White Nile, on average, contributes 23 km^3 of flow into the Nile River each year. This is approximately 25% of the annual Nile flow. Correlation coefficients calculated between the White Nile annual discharge and the eight consecutive quarters of the SST index are shown in Table 5. The results reveal that a maximum of only 4% of the annual variance in the discharge can be explained by ENSO. This correlation is much smaller than that found for the other two major tributaries of the Nile. From these results, it can be concluded that the ENSO signature observed in the Nile discharge measured at Aswan is due entirely to the ENSO dependence of the Blue Nile and Atbara rivers.

4. Discussion

The negative correlation found between the SST anomaly and the annual discharge of the Amazon is consistent with an earlier finding regarding the association between Amazon discharge and monthly mean SST in the eastern and central equatorial Pacific using a cross-spectral analysis (Richey et al., 1989). Previous linear regression analysis on the discharge of the Rio Trombetas has also revealed an association between streamflow in eastern Amazonia and ENSO (Molion and de Moraes, 1987) that is consistent with the results of this study. Flow in the Trombetas River, which eventually joins the Amazon, is positively dependent on the SOI, with the ENSO index leading river flow by about six months (WMO-UNEP, 1992).

The weak negative correlation found between the warm ENSO phase and the annual discharge of the Congo agrees well with the weak positive correlations found between the cold phase and river stage during both seasons of the Congo River flood (Hirst and Hastenrath, 1983). The analysis performed for the Amazon and Congo rivers indicate that flow in these large, equatorial rivers is weakly correlated with ENSO.

The positive correlation observed between the warm phase and Paraná River discharge is in agreement with observations of low discharge in this river during the cold phase (Molion and de Moraes, 1987). The triggering of the 100-year flood of the Paraná by an unusually warm ENSO episode in 1982–83 further demonstrates the teleconnection of ENSO events to climatic anomalies over the southeastern South America region (Depetris and Kempe, 1990). The 100-year Paraná River flood of 1983, nearly double the average annual flood, significantly influences the results of our analysis. Excluding the 1983 flood from the data set reduces the correlation calculated between ENSO and the Paraná River discharge from 20% to 12% variance. However, the anomalously large flood in 1983 associated with the exceptionally warm El Niño episode of 1982 is entirely consistent with the positive correlation observed between river flow and the warm ENSO phase for this river. The annual discharge of the Paraná is clearly associated with ENSO, particularly in the case of extreme ENSO events.

Two major tributaries of the Nile River, the Blue Nile and Atbara, display a significant negative correlation with ENSO. Flow in the White Nile however, was found to show a

weak negative association with ENSO. This analysis confirms the assertion that the coupling between Nile River flow and ENSO is due almost entirely to the Blue Nile and Atbara tributaries of the Nile. The results of our study indicate that the Paraná and Nile rivers, which are smaller and more distant from the equator than the Amazon and Congo rivers, are more strongly correlated with ENSO than the two larger equatorial rivers.

Assuming that river discharge is a linearly dependent function of the SST anomaly, scatter plots similar to those in Fig. 4 have been used to forecast probabilistically the annual discharges of the Nile (Eltahir, 1996) and the Murray rivers (Simpson et al., 1993). Such forecasts of annual discharge were more accurate than assuming the expected river flow to be the long-term average annual discharge. This method could not be used for successful flow prediction in the Amazon and Congo rivers because only weak correlations, smaller by about a factor of two than those calculated for the Nile River, were observed between river discharge and the SST index of ENSO. Probabilistic predictions of the Paraná River discharge were also no better than a forecast of an average annual flood. This failure is due to the fact that the correlation calculated between Paraná River flow and ENSO when excluding the 1983 data point is similar in magnitude to the correlations observed for the Amazon and Congo rivers. While the 1983 flood significantly influences the calculation of correlation coefficients, it is only a single point in the annual flood distribution and therefore does not affect the probability forecast more than any other data point.

An advantage of the method used in this analysis is that it quantifies the percentage of variance in streamflow that can be explained by ENSO. Many other methods of determining a relation between two data sets, such as coherence analysis, do not provide an estimate of the strength of the association that may exist. The results of a homogeneous

Table 6
Summary of ENSO results on riverflow/rainfall for tropical rivers/regions

Region/river	Tendency in ENSO warm phase	Reference
South America		
Amazon River	Reduced discharge	Richey et al. (1989); this work
Trombetas River	Reduced discharge	WMO-UNEP (1992)
Nordeste, Brazil	Reduced rainfall	Chu (1991)
Paraná River (extra tropics)	Enhanced discharge	Molion and de Moraes (1987); this work
Africa		
Nile River	Reduced discharge	Eltahir (1996); this work
Congo River	Reduced discharge	Hirst and Hastenrath (1983); this work
Southeast Africa	Reduced rainfall	Ropelewski and Halpert (1987)
Asia–Australia		
India	Reduced rainfall	Rasmusson and Carpenter (1983); Parthasarathy and Pant (1985)
Murray–Darling Rivers (extra tropics)	Reduced discharge	Simpson et al. (1993)

regression analysis, however, can be used to characterize river discharge by the strength of the association with ENSO. Table 6 summarizes the correlations that were found between the ENSO warm phase and river flows for the Amazon, Congo, Paraná, Nile and other rivers. Also included in the summary are some results on regional rainfall tendencies in tropical areas for which river flow data were unavailable, based on other studies.

Although the correlations between river flow/rainfall and temperature are generally rather weak in the various convective regions, the systematic negative sign of these correlations throughout the tropics is quite remarkable. The only exception in Table 6 is the case of the Paraná, the one river that extends significantly outside the tropics. On average, warmer conditions and elevated surface pressures are associated with reduced rainfall and river discharge throughout the tropical belt. One possible explanation for this behaviour builds directly on ideas developed by G.T. Walker for global scale atmospheric circulations on inter-annual time scales. The warm phase of ENSO is characterized by a strong large-scale atmospheric upwelling in the eastern Pacific Ocean. This upwelling and related low level convergence in the eastern Pacific is likely associated with subsidence and a contribution to low level divergence in all other parts of the tropics. Adiabatic warming in subsidence will contribute to a temperature increase and will also tend to suppress the lifting process necessary for rainfall and river discharge in regions removed from the eastern Pacific upwelling. These ideas have recently been strongly substantiated (Wu, 1996). A similar synoptically controlled relationship between temperature and rainfall is observed in association with the Hadley circulation (Williams et al., 1992).

5. Conclusions

1. The associations between the annual discharges of major tropical rivers and the phase of the El Niño–Southern Oscillation were investigated in this study. It was found that the Amazon and Congo rivers exhibit weak, negative correlations with the SST anomaly of the eastern and central equatorial Pacific, an index of ENSO. This result is consistent with earlier studies of these rivers. The annual discharges of the Nile River and two tributaries of the Nile, the Blue Nile and Atbara rivers, were more strongly correlated to ENSO. The magnitudes and signs of the correlations found for the two Nile tributaries were similar to those calculated for the total Nile discharge. Flow in the third major tributary, the White Nile, exhibited very little dependence on ENSO. The Paraná river was also found to be better correlated with ENSO than the Amazon and Congo rivers. The positive correlation observed for the Paraná River is consistent with other studies of this river. While approximately 20 and 25% of the variance in the annual Paraná and Nile river discharges could be explained by ENSO, respectively, a much smaller correlation on the order of 10% variance due to ENSO was found for the annual discharges of the Amazon and Congo rivers.
2. The four major rivers studied in this paper are correlated by varying degrees to the ENSO index. The Amazon and Congo, which are large rivers close to the equator, exhibit a weak dependence on ENSO, but a consistent tendency for reduced discharge

in the ENSO warm phase. The Nile and Paraná rivers, which produce less annual discharge and are located further away from the equator, display a stronger correlation with the ENSO index, greater by a factor of two than the correlations found for the two larger rivers. This relationship between the strength of the ENSO signal in river discharge and the size and proximity to the equator of tropical rivers is one that requires further research.

3. The Blue Nile and Atbara, but not the White Nile, are responsible for the ENSO signature observed in the total Nile River discharge measured at Aswan.
4. The systematic tendency for reduced tropical rainfall and river discharge in the ENSO warm phase is attributable to global scale subsidence associated with the major upwelling in the eastern Pacific Ocean.

Acknowledgements

The contribution of E.R. Williams to this study has been supported by the NASA Marshall Space Flight Center (H. Christian) and the Climate Dynamics Program at NSF (J. Fein).

References

Cane, M.A., Zebiak, S.E., Dolan, S.C., 1986. Experimental forecasts of El Niño. Nature 321, 827–832.

Chen, D., Zebiak, S.E., Busalacchi, A.J., Cane, M.A., 1995. An improved procedure for El Niño forecasting: implications for predictability. Science 269, 1699–1702.

Chiew, F.H.S., McMahon, T.A., Dracup, J.A., Piechota, T.C., 1995. Climate and streamflow patterns in Australia associated with El Niño/Southern Oscillation (abstract), Eos Trans. AGU, 76 (46).

Chu, P.S., 1991. Brazil's climate anomalies and ENSO. In: Glantz, M.H., Katz, R.W., Nicholls, N. (Eds.), Teleconnections Linking Worldwide Climate Anomalies. Cambridge University Press, Cambridge, ch. 3.

Depetris, P.J., Kempe, S., 1990. The impact of the El Niño 1982 event on the Paraná River: its discharge and carbon transport. Palaeogeog., Palaeoclimatol., Palaeoecol. 89 (3), 239–244.

Eltahir, E.A.B., 1996. El Niño and the natural variability in the flow of the Nile River. Water Resour. Res. 32 (1), 131–137.

Gill, A.E., Rasmusson, E.M., 1983. The 1982–83 climate anomaly in the equatorial Pacific. Nature 306, 229–234.

Hansen, J., Lebedeff, S., 1987. Global trends of measured surface air temperature. J. Geophys. Res. 92, 13 345–13 372.

Hirst, A.C., Hastenrath, S., 1983. Diagnostics of hydrometeorological anomalies in the Zaïre (Congo) basin. Q. J. R. Meteorol. Soc. 109, 881–892.

Kahya, E., Dracup, J.A., 1993. U.S. streamflow patterns in relation to the El Niño/Southern Oscillation. Water Resour. Res. 29 (8), 2491–2503.

Kiladis, G., Sinha, S.K., 1991. ENSO, monsoon and drought in India. In: Glantz, M.H., Katz, R.W., Nicholls, N. (Eds.), Teleconnections Linking Worldwide Climate Anomalies. Cambridge University Press, Cambridge, ch. 14.

Mechoso, C.R., Iribarren, G.P., 1992. Streamflow in southeastern South America and the Southern Oscillation. J. Clim. 5 (12), 1535–1539.

Milliman, J.D., Meade, R.H., 1983. World-wide delivery of river sediment to the oceans. J. Geol. 91 (1), 1–21.

Molion, L.C.B., de Moraes, J.C., 1987. Oscilacao Sul e descarga de rios na America do Sul Tropical. Rev. Bras. de Engenharia, Caderno de Recurso Hídricos 5, 53–63.

Moss, M.E., Pearson, C.R., McKerchar, A.I., 1994. The Southern Oscillation index as a predictor of the probability of low streamflows in New Zealand. Water Resour. Res. 30 (10), 2717–2723.

Parthasarathy, B., Pant, G.B., 1985. Seasonal relationships between Indian summer monsoon rainfall and the southern oscillation. J. Climatol. 5, 369–378.

Parthasarathy, B., Diaz, H.F., Eischeid, J.K., 1988. Prediction of all-India summer monsoon rainfall with regional and large-scale parameters. J. Geophys. Res. 93, 5341–5350.

Quinn, W.H., Zopf, D.O., Short, K.S., Kuo Yang, R.T.W., 1978. Historical trends and statistics of the Southern Oscillation, El Niño, and Indonesian drought. Fish. Bull. 76, 663–678.

Rao, V.B., Hada, K., 1990. Characteristics of rainfall over Brazil: annual variations and connections with the Southern Oscillation. Theor. Appl. Climatol. 42 (2), 81–91.

Rasmusson, E.M., Carpenter, T.H., 1982. Variations in tropical sea surface temperature and surface wind fields associated with the Southern Oscillation/El Niño. Mon. Weather Rev. 110, 354–38.

Rasmusson, E.M., Carpenter, T.H., 1983. The relationship between eastern equatorial Pacific sea surface temperatures and rainfall over India and Sri Lanka. Mon. Weather Rev. 111, 517–528.

Richey, J.E., Nobre, C., Deser, C., 1989. Amazon River discharge and climate variability: 1903–1985. Science 246, 101–103.

Ropelewski, C.F., Halpert, M.S., 1987. Global and regional scale precipitation patterns associated with the El Niño/Southern Oscillation. Mon. Weather Rev. 115, 1606–1612.

Russell, G., Miller, J., 1990. Global river runoff calculated from a global atmospheric general circulation model. J. Hydrol. 117, 241–254.

Shahin, M., 1985. Hydrology of the Nile Basin. Elsevier, Amsterdam, p. 573.

Shea, D., 1986. Climatological Atlas: 1950–1979, Surface Air Temperature, Precipitation, Sea-level Pressure and Sea-Surface Temperature (45°S–90°N). National Center for Atmospheric Research/TN-269 + STR, Boulder, CO.

Simpson, H.J., Cane, M.A., Herczeg, A.L., Zebiak, S.E., Simpson, J.H., 1993. Annual river discharge in southeastern Australia related to El Niño–Southern Oscillation forecasts of sea surface temperatures. Water Resour. Res. 29 (11), 3671–3680.

Trenberth, K.E., Shea, D.J., 1987. On the evolution of the Southern Oscillation. Mon. Weather Rev. 115. 3078–3096.

Williams, E.R., Rutledge, S.A., Geotis, S.G., Renno, N., Rasmussen, E., Rickenbach, T., 1992. A radar and electrical study of tropical "hot towers". J. Atmos. Sci. 49(15), 1386–1395.

WMO-UNEP, 1992. The Global Climate System: Climate System Monitoring, December 1988–May 1991. WMO-UNESCO, Geneva, p. 41.

Wright, P.B., 1989. Homogenized long-period Southern Oscillation indices. Int. J. Climatol. 9, 33–54.

Wu, Z., 1996. The Influence of Sea Surface Temperature on Air Temperature in the Tropics. PhD Thesis, Dept. of Earth Atmospheric and Planetary Sciences, MIT, Cambridge, MA.